High-Precision Measurement of Parity Nonconserving Optical Rotation in Atomic Lead

D. M. Meekhof, P. Vetter, P. K. Majumder, S. K. Lamoreaux, and E. N. Fortson
Department of Physics, FM-15, University of Washington, Seattle, Washington 98195
(Received 23 July 1993)

We have completed a new measurement of parity nonconserving (PNC) optical rotation near the 1.279 μm magnetic dipole absorption line in lead, improving earlier results on this line by a factor of 20. We find the ratio of the PNC $E1$ amplitude to the $M1$ amplitude to be $\mathcal{R} = (-9.86 \pm 0.12) \times 10^{-8}$, consistent with theoretical predictions. Difficulties in the atomic theory of lead presently limit the extent to which our result tests the standard model of electroweak interactions. The amplitude of the nuclear spin-dependent PNC rotation is found to be less than 2×10^{-2} of the nuclear spin-independent rotation.

PACS numbers: 42.50.Wm, 11.30.Er, 35.10.Wb

The standard model of electroweak interactions predicts parity nonconservation (PNC) in atoms caused by the exchange of the neutral Z_0 boson between atomic electrons and quarks in the nucleus [1]. PNC has been measured in a number of heavy atoms [2], with a precision that has reached 2% in cesium [3] and bismuth [4]. Because the effects of atomic structure in the case of cesium have been calculated to an accuracy of 1% [5], cesium PNC has become an especially important probe of electroweak physics [6].

We report here a new measurement of parity nonconserving optical rotation on the 1.28 μm magnetic dipole absorption line in lead vapor that improves our earlier result [7] on this line by a factor of 20, and yields a 1% determination of PNC in the lead atom, the most accurate measurement of atomic PNC to date. This measurement is a major step toward the goal of measuring PNC on a string of separated lead isotopes to cancel the uncertain effects of atomic structure and make a clean atomic test of electroweak physics [8,9]. Of more immediate interest, the same experiment can be carried out on thallium, using a magnetic dipole line at nearly the identical wavelength as lead [10] but for which the size of PNC can be calculated much more reliably [11]. A measurement of PNC in thallium to the accuracy demonstrated with lead should test electroweak theory at the same level as the current cesium results. Also, with this accuracy, it should be possible to observe the nuclear spin-dependent PNC, and thereby measure the anapole moment [12] of the thallium nucleus.

We measure the quantity $\mathcal{R} \equiv \mathrm{Im}(\mathcal{E}_{\mathrm{PNC}}/\mathcal{M})$, where $\mathcal{M}$ is the magnetic-dipole amplitude of the absorption line and $\mathcal{E}_{\mathrm{PNC}}$ is the electric-dipole amplitude coupled into the same line by the PNC interaction within the lead atom. The interference between the two multipoles produces a rotation of the plane of polarized light in the vapor by an angle $\phi_P(\nu) = -4\pi L \nu c^{-1}[n(\nu) - 1]\mathcal{R}$, where ν is the optical frequency, $n(\nu)$ is the refractive index due to the absorption line, and L is the path length. Because $n(\nu)$ follows a dispersion curve, the characteristic frequency shape of $\phi_P(\nu)$ across the absorption line helps to distinguish it from other rotations. Absolute angle calibration is accomplished by separate measurements of $\phi_F(\nu)$, the Faraday rotation [2] associated with the absorption line, using a known magnetic field $\mathbf{B}$ parallel to the light beam.

A schematic diagram of the experiment is shown in Fig. 1. Light from a tunable external cavity InGaAs diode laser at 1.28 μm, with spectral width < 1 MHz, passes through a polarizing calcite prism, a Faraday rotator, a 1 m length of lead vapor, an analyzing calcite prism, a diffraction grating and spatial filter (to remove oven blackbody light), and then enters an InGaAs p-i-n photodiode detector. A fraction of the laser output is sent through a Fabry-Pérot cavity to measure the laser frequency sweep. The Faraday rotator, consisting of a Hoya FR-5 glass rod to which we apply an ac magnetic field at $\omega/2\pi = 1.3$ kHz, modulates the plane of polarization by an angle $\phi_m \cos(\omega t)$, with $\phi_m \sim 10^{-3}$ rad. The intensity of the light transmitted by the analyzing prism is given by $I(\nu, t) = I(\nu) \sin^2[\phi_m \cos(\omega t) + \phi_B(\nu) + \phi_F(\nu) + \phi_P(\nu)]$, where $I(\nu)$ is the transmission line shape due to the lead, and $\phi_B(\nu)$ is any background rotation. In the

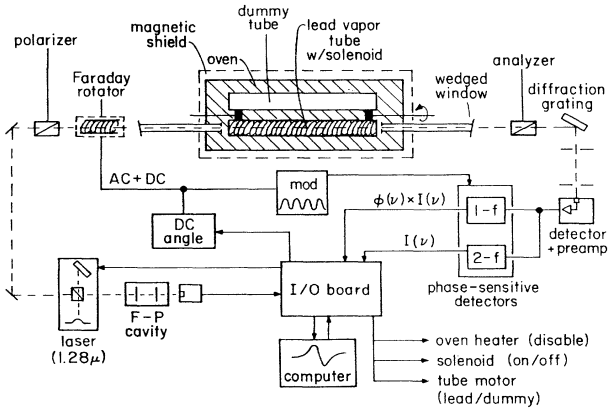

FIG. 1. Block diagram of the experiment.

0031-9007/93/71(21)/3442(4)$06.00

small angle limit appropriate for this experiment, the detected light intensity is thus modulated at 1ω and 2ω, with the 1ω component linear in the optical rotation. We measure both the 1ω and 2ω components with phase sensitive detectors (PSDs) to produce (optical rotation)×(transmission) and pure transmission data.

The oven contains an 8 cm diam ceramic tube fitted with antireflection coated, wedged windows, and filled with buffer gas (about 1 torr of hydrogen and 15 torr of helium). A 1 m region of the tube is heated to between 850 and 1050 °C, to produce a wide range of atomic vapor densities. Spurious wavelength-dependent optical rotations, $\phi_B(\nu)$, of order 1 μrad occur even in the absence of the lead atomic vapor due to interference effects in optical elements between the polarizer and analyzer. To address this problem, two parallel 2.5 cm diam open-ended ceramic tubes are mounted inside the heated tube, one with only the buffer gas, and one containing the lead sample and hot lead vapor confined by the buffer gas. By moving the empty tube into the optical path and scanning the laser frequency, changing no optical components, we obtain background rotation data which can be subtracted from the lead optical rotation data. To control B a molybdenum solenoid is cemented to the ceramic tube containing the lead. The entire oven assembly is surrounded by two layers of magnetic shielding to reduce stray magnetic fields.

Measurements are made by repeatedly sweeping the laser frequency up and down across the transition. The PSD outputs are averaged separately for up and down at 200 frequency points to give laser transmission and (angle)×(transmission) data. A single sweep takes roughly 5 s. A single 10 min measurement cycle includes equal numbers of lead-tube and empty-tube laser sweeps. In addition, during the lead-tube half cycle one or two sweeps are taken with a known applied B (between 10 and 30 mG) and averaged separately to provide lead Faraday rotation data for calibrating the rotation angle. A data run consists of 4 to 8 lead-tube and empty-tube cycles, with the order of the tubes alternating between cycles to reverse the effects of background rotation drifts. Before each run, the optics are readjusted to randomize the shape of the background rotation. Parameters such as the magnetic field for Faraday sweeps, laser sweep speed, and sweep width are also varied between each run. Polarizer orientation, buffer gas pressure, and laser power are varied less frequently. To obtain one data set, data runs at a single optical depth are accumulated over several days until the statistical error in $\mathcal{R}$ is reduced to roughly 1%. We have taken seven data sets at optical depths ranging from 8 to 65 absorption lengths at the central absorption peak.

Lead of natural abundance is used, which produces the transmission profile shown in Fig. 2 for the 1.28 μm transition. The three even isotopes (208,206,204) provide the central absorption peak, and the hyperfine splitting of ^{207}Pb ($I = 1/2$) gives two outer peaks 3.5 GHz apart.

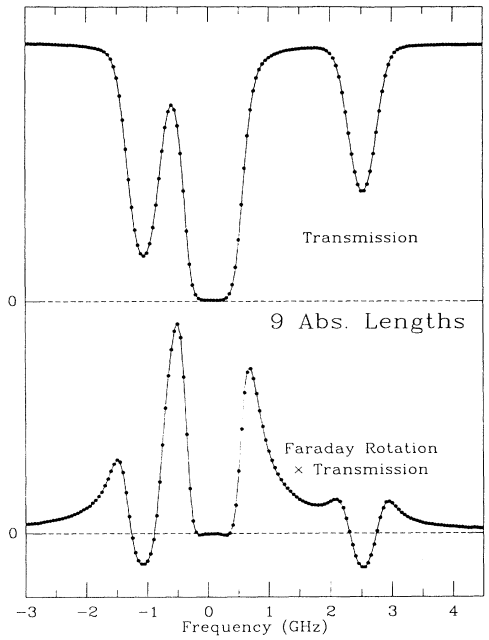

FIG. 2. Transmission and Faraday rotation data and fits (solid lines) from the combined six cycles of a 1 h data run at 9 absorption lengths, as measured at the central absorption peak.

Our analysis benefited from recent precise measurements of both isotope shifts and abundances [13].

Each measurement cycle is analyzed by first fitting the Fabry-Pérot traces with a four term polynomial of frequency versus computer bin number. The theoretical profiles for the transmission, Faraday, and PNC line shapes consist of Doppler- and Lorentz-broadened curves summed over the different isotopes and hyperfine lines. The transmission traces are fit to find line-shape parameters such as the two widths, the optical depth, and laser off-mode light. These parameters are then used to find the fitted amplitude of the Faraday rotation data, which for a known magnetic field and optical depth serves to calibrate the PNC measurement. The typical quality of these fits can be seen in Fig. 2. Finally, the PNC angle data minus the empty tube angle data is fit by $I(\nu)[\phi_F(\nu)+\phi_P(\nu)+\Delta\phi_B(\nu)]$. The transmitted on-mode laser light, $I(\nu)$, is a known function from the transmission line-shape fit. The remaining background rotation which is not successfully subtracted out due to drifting or other effects is denoted here by $\Delta\phi_B(\nu)$, and is modeled as a polynomial in frequency. Inclusion of $\phi_F(\nu)$ allows for Faraday rotation due to any residual magnetic field. Since the Faraday rotation is largely symmetric about each line, it is quite distinguishable from the dispersive PNC line shape. Figure 2 shows a Faraday rotation scan and fit. Figure 3 shows the combined PNC rotation data and fit for the highest absorption length data set.

Two independent methods for absolute angle calibration can be used: mechanical and atomic Faraday. The

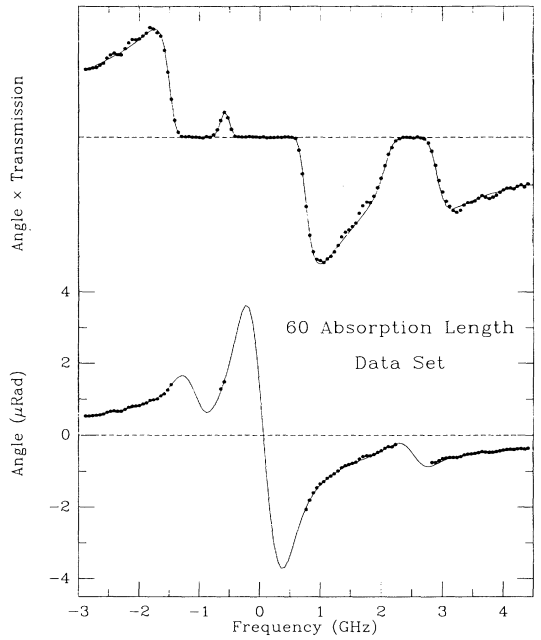

FIG. 3. Combined parity rotation data from the data set at 60 absorption lengths, representing 40 h of data acquisition. The top trace shows (angle)×(transmission) data, as measured and analyzed in the experiment. Below is the same data with the transmission envelope divided out to show the dispersive shape of the pure PNC rotation. Points with very large angle uncertainty, due to near zero light transmission, are omitted. Solid lines represent fitted theoretical profiles.

mechanical calibration is uncertain at the 1% level due to polarizer imperfections and laser beam divergence. The estimated error is based on observed variations as the optical path is changed, and on differences in results using Nicol and Glan-Thompson type calcite polarizers. In the atomic calibration method, uncertainties stem from either the magnetic field determination or errors in the fitting procedure for the Faraday rotation line shapes. Both from measurement of the coil spacing, and from explicit magnetometer measurements, the magnetic field uncertainty was estimated to be less than 0.3%. While small systematic line-shape errors exist in the Faraday fit, these errors largely cancel in determining $\mathcal{R}$, since $\mathcal{R}$ is found from the ratio between the PNC fit and Faraday fit amplitudes. The determination of $\mathcal{R}$ using the mechanical calibration does not take advantage of this cancellation. Overall, the atomic Faraday calibration contributes a smaller error than the mechanical method, and is used to obtain the final value of $\mathcal{R}$. We also compute a mean value and uncertainty using the mechanical method to demonstrate the agreement of the analyses. The atomic Faraday calibration uncertainties (other than uncertainty in the magnetic field) are most naturally included as part of the line-shape systematic error in the analysis summarized below.

Data were averaged by cycle, by run, and by day to search for evidence of nonstatistical scatter due, for example, to the projection of $\Delta\phi_B(\nu)$ onto the PNC fits. While mean values for $\mathcal{R}$ agreed very well in all cases, the day-to-day scatter of $\mathcal{R}$ was slightly larger than what the cycle-to-cycle scatter would imply ($\chi^2 \sim 2$), which is consistent with other evidence that $\Delta\phi_B(\nu)$ varies more slowly than the data cycle period. Final statistical uncertainties assigned to a given data set are based on the larger scatter. We investigated potential correlations by performing linear fits of $\mathcal{R}$ with numerous other fit parameters and operating condition variables tabulated for each individual data cycle. In a few cases, resolved correlations contributed significantly to the observed scatter, but in no case did a resolved correlation indicate the need for extrapolating $\mathcal{R}$ beyond the statistical error. The observed correlations can be explained by the effects of $\Delta\phi_B(\nu)$ or by the systematic effects discussed next.

The most important class of systematic errors involved uncertainties in the fitting functions. In exact background subtraction, drifting magnetic fields, small laser sweep nonlinearity, as well as imprecisely modeled atomic line shapes could all lead to fitting errors and possible systematic errors in $\mathcal{R}$. To place limits on the systematic uncertainties associated with each of these issues, we reanalyzed a large, representative subset of our data using many appropriately altered fitting procedures. One such test was to compare results when the data were fit using different weighting functions emphasizing different portions of the absorption line. This test was especially important since the residuals of our line-shape fits revealed small statistically resolved systematic features (between 0.1% and 1% of the signal size) which varied across the line. Data were also fit with $\Delta\phi_B$ modeled as either a constant, a linear, or a quadratic function of frequency. In the extreme case, these refits resulted in Faraday calibration changes of 4%. However, in all cases a simultaneous change in the PNC line-shape fit resulted in a final value for $\mathcal{R}$ which varied by no more than 1%, and was more typically less than 0.3%. It is easy to see why this partial "cancellation" of systematic shifts occurs. Consider, for example, a small error in the optical depth determined by an improper fit to the transmission line shape. Since both the Faraday and PNC line shapes scale linearly with this quantity, what might at first appear to lead to calibration uncertainty has no effect on the final value of $\mathcal{R}$. This argument applies in some degree to many aspects of the line-shape fitting procedure. When $\Delta\phi_B$ was modeled as a linear function, rather than a constant term, we found a significant change in $\mathcal{R}$ only for the case of lowest absorption length, where background subtraction failures would have the largest possible systematic effect. In all cases the subsequent inclusion of a quadratic term changed the final results by less than 1 standard deviation.

Figure 4 summarizes the results of the seven data sets. The fractional statistical uncertainty of the combined data is 0.4%. It is particularly encouraging that we find

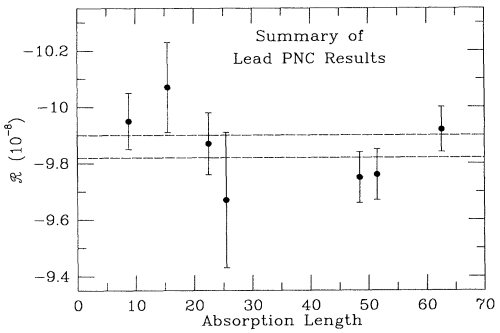

FIG. 4. The value of $\mathcal{R}$ plotted versus absorption length for the seven data sets. The error bars show statistical uncertainties only, yielding a χ^2 of 1.1. The horizontal dashed lines represent the $\pm 1\sigma$ uncertainty of the combined weighted average.

no dependence of $\mathcal{R}$ on optical depth over nearly an order of magnitude change in ϕ_P. Potential systematic errors in $\mathcal{R}$ would almost certainly not scale exactly as ϕ_P and would appear, on a plot such as this, as nonstatistical variations of $\mathcal{R}$ with optical depth. Based on consideration of the residual line-shape misfits, the variation in $\mathcal{R}$ resulting from refitting data, and uncertainty in the calibration magnetic field, we assign a fractional systematic error of 1.1%. Using the atomic Faraday calibration method, the final value of the PNC optical rotation in lead (normalized to ^{208}Pb) is then

$$\mathcal{R} = (-9.86 \pm 0.04 \pm 0.11) \times 10^{-8}.$$

Using instead the mechanical calibration method we find $\mathcal{R} = (-9.81 \pm 0.25) \times 10^{-8}$, which, though less precise, agrees well with the above value.

Our experimental result in lead does not at present provide an exacting test of electroweak theory. Theoretical predictions for $\mathcal{R}$ agree well with our result, but due to the complicated electronic structure in lead, are uncertain at the 8% level [11]. We can determine a value of the weak charge [2], $Q_w(^{208}\mathrm{Pb}) = -114 \pm 9$, where the error is due to atomic theory. A nuclear spin-dependent PNC effect in lead ($\mathcal{R}_{\mathrm{SD}}$) would appear as dispersive optical rotation of opposite sign on the two hyperfine components of the odd isotope ^{207}Pb. Such effects are suppressed by a factor of Q_w relative to the spin-independent rotation, and theoretical predictions for this effect in lead are particularly small [14]. By fitting explicitly for the spin-dependent line shape we are able to set the upper limit $\mathcal{R}_{\mathrm{SD}}/\mathcal{R} < 0.02$ (95% confidence), where here $\mathcal{R}$ refers to the spin-independent rotation of the ^{207}Pb, $F = 1/2 \rightarrow 3/2$ hyperfine line.

Because of potential difficulties in improving lead atomic structure calculations, our result is perhaps best viewed as a proof of experimental principle. Work now under way in thallium [10] should lead to experimental results of equal precision in a system where the potential for accurate atomic structure calculations is much greater. Furthermore, well-resolved hyperfine components in the $I = 1/2$ thallium isotopes should facilitate a measurement of the spin-dependent anapole moment [12], predicted to be relatively large for this element. Finally, future plans include the measurement of PNC in a number of separated isotopes of lead. Comparing isotopic differences in $\mathcal{R}$ to theoretical predictions eliminates atomic structure uncertainties in the calculations. Remaining uncertainties due to nuclear structure isotopic differences are being studied [9,15]. Measurements of hyperfine or isotopic differences such as these will be free of uncertainties in absolute angle calibration, as well as certain line-shape systematics which would be common to all transitions. Therefore such measurements could be much more precise than the present results, and should provide important new tests of physics of (and beyond) the standard model.

We would like to thank J. M. Reeves and T. D. Wolfenden for assistance at an earlier stage of the experiment, and B. Nelson for isotopic abundance determination. This work is supported by National Science Foundation Grant No. PHY-9206408.

[1] M.A. Bouchiat and C.C. Bouchiat, Phys. Lett. **48B**, 111 (1974).
[2] E.N. Fortson and L.L. Lewis, Phys. Rep. **113**, 289 (1984); E.A. Hinds, in *Atomic Physics 11*, edited by S. Haroche, J.C. Gay, and G. Grynberg (World Scientific, Singapore, 1989), p. 151; D.N. Stacey, Phys. Scr. **40**, 15 (1992).
[3] M.C. Noecker, B.P. Masterson, and C.E. Wieman, Phys. Rev. Lett. **61**, 310 (1988).
[4] M.J.D. Macpherson, K.P. Zetie, R.B. Warrington, D.N. Stacey, and J.P. Hoare, Phys. Rev. Lett. **67**, 2784 (1991).
[5] S. A. Blundell, W. R. Johnson, and J. Sapirstein, Phys. Rev. Lett. **65**, 1411 (1990)
[6] M. E. Peskin and T. Takeuchi, Phys. Rev. D **46**, 381 (1992).
[7] T.P. Emmons, J.M. Reeves, and E.N. Fortson, Phys. Rev. Lett. **51**, 2089 (1983).
[8] V.A. Dzuba, V.V. Flambaum, and I.B. Khriplovich, Z. Phys. D **1**, 243 (1986); C. Monroe, W. Swann, H. Robinson, and C.E. Wieman, Phys. Rev. Lett. **65**, 1571 (1990).
[9] E.N. Fortson, Y. Pang, and L. Wilets, Phys. Rev. Lett. **65**, 2857 (1990); S.J. Pollock, E.N. Fortson, and L. Wilets, Phys. Rev. C **46**, 2587 (1992).
[10] P. Vetter, D.M. Meekhof, P.K. Majumder, S.K. Lamoreaux, and E.N. Fortson, Bull. Am. Phys. Soc. **38**, 1121 (1993); T.D. Wolfenden, P.E.G. Baird, and P.G.H. Sandars, Europhys. Lett. **15**, 731 (1991)
[11] V.A. Dzuba, V.V. Flambaum, P.G. Silvestrov, and O.P. Sushkov, Europhys. Lett. **7**, 413 (1988).
[12] I.B. Khriplovich, Commun. At. Mol. Phys. **23**, 189 (1989), and references therein.
[13] J.M. Reeves, and E.N. Fortson, Phys. Rev. A **44**, R1439 (1991); B. Nelson (private communication).
[14] I.B. Khriplovich, *Parity Nonconservation in Atomic Phenomena* (Gordon and Breach, Philadelphia, 1991).
[15] B. Chen and P. Vogel (to be published).